

## **Title**

Differences in physiology explain succession of mixoplankton functional types and affect carbon fluxes in temperate seas

## **Authors**

Suzana Gonçalves Leles<sup>1,2\*</sup> (suzanaleles@gmail.com), Jorn Bruggeman<sup>1</sup> (jbr@pml.ac.uk), Luca Polimene<sup>1</sup> (luca@pml.ac.uk), Jerry Blackford<sup>1</sup> (jcb@pml.ac.uk), Kevin J Flynn<sup>1</sup> (kjf@pml.ac.uk) and Aditee Mitra<sup>3</sup> (MitraA2@cardiff.ac.uk)

<sup>1</sup>Plymouth Marine Laboratory, Prospect Place, Plymouth, PL1 3DH, UK, <sup>2</sup>Biosciences Department, Swansea University, Singleton Park, Swansea, SA2 8PP, UK, <sup>3</sup>School of Earth and Ocean Sciences, Cardiff University, Park Place, Cardiff, CF10 3AT, UK

**\*Corresponding author:** suzanaleles@gmail.com

**Running title:** On the seasonal succession of mixoplankton

**Keywords:** Functional type, seasonal succession, ecosystem functioning, carbon cycling, plankton, protists, mixotrophy

## **Statement of authorship**

All authors designed the study. SGL and JBr wrote the model code. SGL ran the simulations, analysed results, prepared figures and wrote the first version of the manuscript. All authors discussed the results and contributed to the final version of this manuscript.

## **Data accessibility statement**

The L4 observational data can be obtained at <https://www.westernchannelobservatory.org.uk/> and the model set up is archived in <https://github.com/suzanaleles/L4-mixo> (Zenodo DOI will be generated after the review process).

**Colour should not be used for any figures in the printed version of this article.**

**Authors have no competing interests to declare.**

## Abstract

Different hypotheses have been proposed explaining plankton community assembly and how changes in biodiversity can impact ecosystem function. Mixoplankton (photo-phago-trophs) are important members of the plankton, but science lacks a clear understanding of their role in plankton succession. Here, we used a modelling approach to test the hypotheses that: i) differences in the physiology of mixoplankton functional types (MFTs) explain their seasonalities and ii) functional differences affect their roles in key carbon fluxes. Functional differences were modelled based on cell size and whether mixoplankton possess their own, or acquire, photosystems. Ecosystem simulations incorporated realistic environmental variability and were validated against a 9yr long-term time series of nutrients, chlorophyll-a, and plankton data from a coastal temperate sea. Simulations, consistent with empirical data, show that mixoplankton of different sizes are present throughout the water column and over time, with seasonal population dynamics differing among the different MFTs. Importantly, the partitioning of production among different size-classes depends on how mixoplankton functional diversity is described in the model, and that merging mixoplankton into one functional type can mask their diverse ecological roles in carbon cycling. Mixoplankton thus play an important role in structuring the plankton community and its dynamics in the simulations.

## 1. Introduction

How changes in biological communities affect ecosystem functioning is a central question in ecology (Chapin et al., 1997). In order to assess this question, it is critical to understand how biological communities interact with their environment (Weithoff and Beisner, 2019). Microbial assemblages display diverse lifestyles which are challenging the way we understand the cycle of carbon in the oceans (Litchman et al., 2007; Mitra et al., 2014; Worden et al., 2015). Mixotrophy – a fusion of autotrophic and heterotrophic nutrition – is a widespread strategy the importance of which has been overlooked across different ecological systems (Selosse et al., 2017). Heterotrophy in microbial protist mixotrophs may be facilitated by osmotrophy and/or phagotrophy. Since all microbes have potential for osmotrophy, here we reserve “phytoplankton” for organisms incapable of phagotrophy, “protozooplankton” for those incapable of phototrophy, and “mixoplankton” for those capable of both photo- and phago- trophy (see also Table 1 of Flynn et al., 2019).

Traditionally, protist plankton were viewed as ‘producers’ or ‘consumers’. In reality, many aquatic protists are mixoplankton, combining both phototrophy and phagotrophy in a single cell (Flynn et al., 2013; Flynn et al., 2019). While the importance of mixotrophy is commonly associated to nutrient-limited environments (Stoecker et al., 1987; Tittel et al., 2003; Zubkov and Tarran, 2008), global analyses revealed the ubiquity of mixoplankton across different spatio-temporal scales in the oceans (Leles et al., 2017; Edwards, 2019; Faure et al., 2019; Leles et al., 2019), suggesting that they can occupy different ecological niches (Leles et al., 2018; Anschütz and Flynn, 2020). The challenge now is to better understand the mechanisms that allow mixoplankton to thrive in contrasting ecosystems (Hansson et al., 2019).

At the eco-physiological level, functional differences could explain the success of mixoplankton under a range of environmental conditions (Stoecker et al., 2017). While mixoplankton differ according to cell size, critically they also differ with respect to the means by which they acquire energy and nutrients (Flynn and Mitra, 2009; Mitra et al., 2016; Flynn et al., 2019). In the late 1980s, field observations revealed that mixoplankton might or not possess their own photosystems (Bird and Kalf, 1986; Stoecker et al., 1987). More recently, their functional classification has been revisited and different mixoplankton functional types (MFTs) have been proposed (Mitra et al., 2016). Functional types, often formed by organisms of quite different taxonomic relationships, are grouped together according to their perceived role in ecology (Blondel, 2003). A combination of cell size and the fundamental difference between innate (constitutive) and acquired (non-constitutive) phototrophy are clear candidates upon which to base functional type descriptions of mixoplankton in models. Here, we model different MFTs to investigate their role in plankton succession and in key carbon fluxes.

A basic distinction can be made between mixoplankton that possess their own photosystems, i.e., constitutive mixoplankton (CMs), and those that need to acquire phototrophic capacity from their photosynthetic prey, i.e., non-constitutive mixoplankton (NCMs) (Mitra et al., 2016). Constitutive forms do not necessarily need to engage on both phototrophy and phagotrophy to grow and/or to survive (Caron et al., 1993; Adolf et al., 2006; Wilken et al., 2013) and can obtain both limiting nutrients or carbon through mixotrophy (Zubkov and Tarran, 2008; Czepionka et al., 2011). In contrast, non-constitutive forms rely on the prey from which they acquire phototrophic ability to survive and the specificity of the prey may affect their success in the environment (Leles et al., 2018). While generalist NCMs rely on diverse prey types, they have lower control over phototrophy and shorter plastid retention times when compared to specialist NCMs (McManus et al., 2012;

Moeller et al., 2016). One can then consider (functional) diversity among mixoplankton functional types, particularly in modelling studies (Leles et al., 2018; Anschütz and Flynn, 2020).

Temperate seas are ideal systems to study plankton succession due to the wide variations in light and temperature gradients resulting in the seasonal stratification of the water column (Sommer et al., 2012). While traditionally envisaged as a result of physical factors, grazing, and nutrient/food limitation (Margalef, 1978; Sterner, 1989; Calbet, 2001), plankton succession is also influenced by other ecological interactions, including mixotrophy (Sommer et al., 2012; Stoecker et al., 2017; Atkinson et al., 2018). Methodological limitations have hindered empirical investigations that account for mixoplanktonic activity when evaluating the seasonal succession of protists and these tend to consider only specific groups of mixoplankton, such as dinoflagellates (Barton et al., 2013; Gran-Stadniczeňko et al., 2019). On the other hand, numerical models can shed light into protist succession allowing for the description of mixotrophy (Troost et al., 2005; Bruggeman, 2009; Mitra & Flynn 2010; Mitra et al., 2014; Berge et al., 2017; Ghyoot et al., 2017). Nevertheless, ecosystem modelling studies that represent the diversity of functional forms observed among mixoplankton whilst incorporating realistic environmental variability (i.e., temperature, light, and mixing) have not yet been applied to explain time series field data.

Here, we tested the hypotheses that differences in physiology explain seasonality in MFTs and that these functional differences affect their roles in key carbon fluxes. The mechanisms driving the seasonal succession of protist trophic strategies (i.e., between phytoplankton, protozooplankton and mixoplankton, defined as per Flynn et al., 2019) were explored using a plankton ecosystem model applied in a coastal stratified temperate sea, the Western English Channel at station L4. The plankton food web was based on plankton functional types and coupled to a 1D model of the water column. Based on previous modelling results that showed different mixoplankton dominating under different light and nutrient regimes (Leles et al., 2018; Anschütz and Flynn, 2020), different mixoplankton functional types were included in the model. The physical model is key to addressing this question since it explicitly represents depth and incorporates realistic environmental variability. We then investigated the ecological roles of mixoplankton within carbon cycling in temperate seas.

## 2. Material and Methods

### 2.1 The ecosystem model

The ecosystem model was built by incorporating a flexible sub-model description of different protist nutrition modes, including mixotrophy (Flynn and Mitra, 2009; Mitra et al., 2016), into the European Regional Seas Ecosystem Model – ERSEM (Blackford et al., 2004; Butenschön et al., 2016), as previously described in Leles et al., (2018). The ecosystem model considers the major elements in the ocean, i.e., carbon, nitrogen, phosphorus, and silicate, both in organic and inorganic forms, accounting for variable stoichiometry among plankton groups (except for mesozooplankton where C:N:P was held constant in the model). Here, the ecosystem model was coupled to a 1D physical model of the water column through the General Ocean Turbulence Model (GOTM; Burchard et al., 1999).

The model includes inorganic nutrients (nitrate, ammonium, phosphate, silicate, dissolved inorganic carbon), dissolved organic matter (DOM), and detrital particulate organic matter (POM). DOM is divided between labile and semi-labile assuming that the former is

rapidly consumed by bacteria and that the latter is more resistant to microbial degradation (Hansell, 2013), while detrital POM is divided in three size-classes. Plankton functional types include two phytoplankton (picophytoplankton and diatoms), three mixoplankton (including constitutive and non-constitutive forms), three zooplankton (nano- and micro- protozooplankton, and mesozooplankton), and one decomposer representing heterotrophic bacteria (see Fig. S1 in Supporting Information). Plankton growth dynamics result from the balance of gains through uptake of nutrients and assimilation into organic compounds and losses through respiration, excretion (non-assimilated material) and/or release of excess of nutrients (linked to stoichiometric regulation), predation, and non-predatory mortality (see Supporting Text). The model does not describe osmotrophy, and thus we do not consider mixotrophy expressed by phytoplankton such as diatoms using DON. For avoidance of doubt, we reserve “mixotrophy” solely for generalised comments, using “mixoplanktonic activity” otherwise. Model equations can be found in full in Leles et al. (2018).

## 2.2 Functional diversity: mixoplankton functional types

The representation of mixoplankton within food webs increases the number of trophic interactions as well as the complexity of the competitive interactions between organisms (Stoecker et al., 2017). However, mixoplankton are not all equal and incorporating functional differences shows how these interactions can change. Furthermore, they can adjust their balance between phototrophic and phagotrophic nutrition according to environmental conditions and organism’s nutritional requirements (e.g., Caron et al., 1993; Schoener and McManus, 2017). Thus, different functional types of mixoplankton exhibit different acclimation responses (Flynn and Mitra, 2009); this is most apparent between CM and NCM forms (Mitra et al., 2016; Flynn et al., 2019), where the latter depends on acquisition of phototrophy from their phototrophic (phytoplanktonic or mixoplanktonic) prey.

In the model, constitutive (CM) forms are assumed to i) take up external inorganic nutrients, ii) rely on phototrophy for a critical proportion of growth, iii) photoacclimate through the synthesis of chlorophyll, and iv) down-regulate the digestion of prey if enough carbon is obtained through phototrophy. Non-constitutive (NCM) forms are assumed to i) not take up external inorganic nutrients, though they can recycle internally regenerated nutrient; ii) rely mainly on phagotrophy for growth (but are obligate mixotrophs, i.e., relying on both food and light to achieve positive growth); iii) obtain phototrophic capacity from their prey and do not photoacclimate and iv) digest prey independently of photosynthesis and egest kleptochloroplasts over time (McManus et al., 2012; Schoener and McManus, 2017). The non-constitutive mixoplankton (NCMs) modelled here are generalists and represent species such as those within the genus *Strombidium*, which have lower control over the acquired phototrophic machinery compared to other NCMs, e.g., *Mesodinium* (Johnson et al., 2013; Moeller et al., 2016). Although both specialist and generalist NCMs were included in the model in our preliminary simulations (since both functional types are found at L4 station), the former could not persist in the model (i.e., were driven to extinction) and, therefore, were not included in our final model.

## 2.3 The plankton food web

It was assumed that nano-protozooplankton feed on pico- and nano- sized prey, micro-protozooplankton feed on pico-, nano-, and micro- sized prey, and mesozooplankton feed on nano- and micro- sized prey (Fig. S1). Different mixoplankton functional types were considered in the model (Fig. S1). Phototrophic nanoflagellates and microflagellates are constitutive mixotrophs (CMs) because they possess their own photosystems (Mitra et al., 2016) and will be referred herein as nano-CMs and micro-CMs, respectively. As supported by

evidence from the literature, they were allowed to feed on the same prey as their heterotrophic counterparts of same size, i.e., the nano-protozooplankton and the micro-protozooplankton, respectively (e.g., Zubkov and Tarran, 2008; Hansen, 2011; Unrein et al., 2007).

In turn, the functional group traditionally ascribed to “microzooplankton” group was divided into strict heterotrophic species (referred herein as protozooplankton) and non-constitutive mixoplankton (Mittra et al., 2016) based on previous estimates suggesting that a large proportion of total microzooplankton are mixoplankton thus acquiring phototrophic potential from their prey (Leles et al., 2017). In the model, NCMs were assumed to obtain phototrophic potential from nano-CMs. Micro-sized protozooplankton and NCMs share the same prey items and were assumed not to feed on each other (Fig. S1). While the latter may not always hold true for real systems, this assumption was necessary to allow their persistence in the model, as revealed by initial numerical experiments. Finally, intraguild predation was allowed among all predators due to its importance in plankton trophodynamics (e.g., Hansen, 2011). Details on how the different plankton groups interacted with the nutrient pools can be found in the online Supporting Text (Figs. S1 and S2).

## 2.4 Model set-up and skill assessment

The ecosystem model was embedded within the water column model GOTM, configured to represent the L4 station. The L4 station is located 13 km SSW of Plymouth, in the Western English Channel, UK (50° 15'N, 4° 13'W; Fig. S3), with a mean water depth of 50 m (Smyth et al., 2010). GOTM was set to resolve 100 vertical layers with increasing resolution towards surface waters and assuming a water column of 50 m depth. The biogeochemical model was run over a period of 9 years (2006–2014; coinciding with the period of the observational data) after a 2-year spin-up period and model output was recorded daily. The model was initialised with *in situ* measurements of temperature, salinity, and inorganic nutrient concentrations observed during winter at L4 (e.g., nitrate = 9  $\mu$ M, phosphate = 0.5  $\mu$ M, silicate = 4.5  $\mu$ M, ammonium = 0.1  $\mu$ M; Smyth et al., 2010) and implemented using the ERSEM benthic coupling, following Butenschön et al. (2016).

The L4 observational data used here includes temperature, salinity, inorganic nutrients, chlorophyll-a, and carbon biomass of all plankton functional types included in the food web model (Smyth et al., 2010; Widdicombe et al., 2010; Atkinson et al., 2015; Tarran and Bruun, 2015). Plankton data were obtained (quasi) weekly at 10 m depth and used to validate simulations from January 2006 to December 2014. Mixoplankton taxa were assigned to different functional types based on species name (Table S1) according to previous reviews (Flynn et al., 2013; Leles et al., 2017, Faure et al., 2019; Leles et al., 2019). Further details of the model set-up (configurations applied to GOTM and the ecosystem model, including model coupling and accessibility), observational data (characterization of L4 station, data collection and data analysis), and model parameterization (calibration experiments and parameter values) are given in the Supporting Text (Tables S2–S5).

Model validation was initiated by comparing simulations with observational data over the whole studied period (i.e., 9 years). Then model output was averaged by month of every year and then averaged again over the years so that climatological means could be obtained. By doing that, we were able to test our hypothesis that differences in physiology explain seasonality in MFTs. To assess model skill, the correlation coefficient, the root mean squared error (RMSE), and the average error (AE) were computed and interpreted through target diagrams. The metrics provided in the target diagrams were the normalised average error (AE\*) in the abscissa and the normalised and unbiased RMSE (RMSE\*) in the ordinate (Jolliff et al., 2009). The model was also compared against standard ERSEM simulations to

evaluate how well our model can predict observational data compared to an established ecosystem model which has been previously tested in different oceanographic regimes (Blackford et al., 2004). ERSEM parameter values conform to the configuration presented in Butenschön et al. (2016).

To test our second hypothesis, that MFT's affect carbon fluxes, we performed a series of extra modelling experiments. Specifically, we compared carbon fluxes obtained from our simulation against model runs that accounted for two, one, or none of the three MFTs included in the reference model. The Supporting Text provides further details on model skill assessment and analysis of the seasonal succession of protist trophic strategies.

### 3. Results

#### 3.1 Model validation

The model reliably reproduced the observed seasonal evolution of inorganic nutrients, chlorophyll-a, and total plankton biomass at L4 (Figs. 1 and S4). The model performed at least as well as ERSEM and, contrary to the latter, captured the biomass of nano-CMs during summer (Figs. S4 and S5 and Table S6). Our results revealed that seasonal dynamics differ among the different mixoplankton functional types, with nano-CMs being the most abundant, micro-CMs being important at occasions, and NCMs being present at low biomass levels throughout the year at L4 (Fig. 1b). Overall, correlations were higher than 0.7 (except for phytoplankton and micro-CMs), simulations do not show significant bias, and the standard deviation of the model was larger ( $RMSE^* > 0$ ) than the reference field's standard deviation (Fig. 1a). Simulations were also able to quantitatively represent the biomass of phytoplankton, mixoplankton, and protozooplankton (Fig. 1b). The model successfully captured the seasonal distribution of nano-CMs and NCMs, but the simulated biomass peak of micro-CMs was earlier than predicted by observations (Fig. 1b).

Model and data revealed the presence of mixoplankton across the seasonal cycle and over depth (Figs. 1b and 2a). Overall, the model agrees with expectations within temperate seas: phytoplankton dominate biomass during the spring bloom and protozooplankton during early winter (Fig. 2a). Mixoplankton dominate once the water column is stratified, but the protist community also shifts from being dominated by protozooplankton to mixoplankton from early to late winter (Fig. 2a); this is also supported by data, although to a lesser extent (Fig. 1b). However, the model overestimates the phytoplankton biomass (notably diatoms) during the spring bloom (Figs. 1b and S4); the standard (non-mixoplankton) variant of ERSEM shows an equal if not greater anomaly in this respect. Below the mixed layer, light attenuation (Fig. S6) decreases the relative importance of phytoplankton (Fig. 2a). It is noteworthy that biomass at deeper levels might not be viable in the model (due to negative net growth) and is more likely to have been brought by turbulent mixing.

#### 3.2 On the succession of mixoplankton functional types

Bottom-up and top-down controls (i.e., simulated growth and predation rates) were evaluated within the mixed layer to understand shifts in plankton community composition in the model (Fig. 2b). At stratification onset, protist growth rates tend to be higher than losses due to predation and, under these conditions, mixing, light, and inorganic nutrients availability favours diatom growth (Figs. 2b). Micro-CMs compete with diatoms for light and inorganic nutrients, but simultaneously predate on diatoms; accordingly, suppression of the diatom bloom due to silicate limitation is followed by the suppression of micro-CMs (Fig.

S7). During summer, the water column is stratified (Fig. S6) and inorganic nutrients and prey are more limiting; much of the spring production has been exported to deeper waters (~ 45% of the total nitrogen within the first 25 meters) and nutrient-nitrogen levels do not increase until autumn due to the presence of the thermocline (Figs. 2a and S6). Such conditions favour picophytoplankton and various mixoplankton (nano-CMs and NCMs; Figs. 2 and S7), with a tight coupling between growth and predation rates being observed (Fig. 2b). During the autumnal breakdown of stratification, diatoms return but do not attain concentrations observed during spring; micro-CMs concentrations remain low, being outcompeted by protozooplankton and NCMs (Fig. S7). Nano-CMs could maintain biomass values similar to those observed during summer (Fig. S7). After the autumn bloom, the water column becomes fully mixed (Fig. S6) and protozooplankton attain their highest contribution to total protist biomass (Fig. 2a). Intense mixing and light limitation result in slow growing populations subjected to high predation pressure (Fig. 2b). Late in winter, phototrophs achieved higher growth rates, predation is relaxed and nano-CMs dominate the mixoplanktonic community (Fig. 2b).

The balance between phototrophic and phagotrophic nutrition differs among the diverse mixoplankton functional types over the simulated seasonal cycle (Fig. 3). Phagotrophy was important to nano-CMs during summer but even more important during winter (Fig. 3). In turn, the relevance of phagotrophy among micro-CMs was significantly related to the availability of suitable prey, i.e., diatoms, which bloom during spring in the model (Fig. 3). A distinction can be seen between CMs and NCMs since the former are primarily phototrophic and the latter are primarily phagotrophic (Fig. 3). Among NCMs, the importance of phototrophy was highest during summer followed by the stratification onset (Fig. 3).

### 3.3 On the roles of mixoplankton in carbon fluxes

We compared model runs that accounted for only one or two MFTs, against observational data at L4 (Figs. S8 and S9). When compared against our reference model (nano-CMs + micro-CMs + NCMs; Fig. 1a), these models performed similarly for nutrients and total chlorophyll but not for protist biomass (Figs. S8 and S9), in which the reference model performed better. Indeed, simulated carbon fluxes in the reference model differed substantially from model runs in which none, one or two MFTs were considered (Figs. 4 and 5). Carbon fluxes were considerably different in the absence of nano-CMs. Specifically, a higher proportion of gross primary production was assigned to smaller size fractions when photo-phago-trophy was not represented among phototrophic nanoflagellates (Fig. 4). Consequently, the simulated mixoplankton community played a minor role in the consumption of heterotrophic bacteria and picophytoplankton (Fig. 5). When all MFTs were removed, only diatoms and picophytoplankton contributed to phytoplankton biomass, with phototrophic nano- and micro- flagellates not persisting in the model.

The impact of herbivory on picophytoplankton is also decreased in the absence of micro-CMs (Fig. 5) because nano-CMs outcompeted the smallest primary producers in the model. Even though diatoms were consumed by micro-CMs and NCMs (but not nano-CMs) in the model, the impact of grazing by mixoplankton on diatoms also decreased if nano-CM activity was not considered (Fig. 5) due to the accumulation of biomass within picophytoplankton. A considerable decrease in the production of labile DOC and in the trophic transfer of carbon to higher trophic levels was observed in the absence of nano-CMs and, consequently, in the vertical export of particles which, in the model, is controlled by sinking of material egested and excreted by mesozooplankton (Fig. 5). Interestingly, contrasting results were found when only nano-CMs and NCMs, and not micro-CMs, were



simulated. Under this scenario, the high biomass achieved by diatoms promoted an increase in the trophic transfer to mesozooplankton and vertical export of carbon (Fig. 5). The contribution of NCMs to key carbon fluxes was not as significant as that of the other groups due to their low biomass observed at L4 (Fig. 5). Mixoplankton thus play an important role in structuring the plankton community and its dynamics in the simulations.

#### 4. Discussion

Our model show, consistent with empirical evidence, that mixoplankton of different types are present over time and across depth within temperate seas (Fig. 1). In the model, functional differences help explain how the balance between phototrophic and phagotrophic nutrition varies according to environmental conditions through the representation of constitutive and non-constitutive mixoplankton and their different trophic interactions (Figs. 2 and 3). Furthermore, seasonal population dynamics differ among different mixoplankton functional types (MFTs; Fig. 1). Not considering these different groups gives a poorer simulation with consequential impacts on carbon fluxes.

Despite being commonly pictured as a strategy to cope with stress under limited inorganic nutrient availability, empirical evidence has shown that mixoplankton can have different ecological niches, comprising a significant fraction of plankton biomass under contrasting environmental conditions (Czypionka et al., 2011; Vargas et al., 2012). Nevertheless, understanding their ubiquity in the oceans has proved to be challenging (Leles et al., 2017; Edwards 2019; Faure et al., 2019; Leles et al., 2019). This has been largely due to the absence of suitable models of MFTs placed within a suitable physical description. Here, we show that accounting for the functional differences among mixoplankton (through the description of different MFTs) is key to better understand their dynamics. In the absence of different MFTs, a different view of the partitioning of primary production among size-classes is given (Fig. 4). Major differences were observed if mixoplanktonic activity was omitted among phototrophic nanoflagellates; it resulted in the underestimation of the contribution of larger size classes to total production (Fig. 4) and masked the potential ecological roles of mixoplanktonic assemblages in carbon cycling (Fig. 5).

#### 4.1 MFTs have different seasonalities and trophic linkages in temperate seas

The modelling framework used here invokes realistic environmental variability and different MFTs in a plankton food web to investigate both competitive outcomes and top down controls in the seasonal succession of protist trophic strategies. Doing so, the model successfully predicts the successional sequence of diverse trophic strategies within temperate seas as well as realistic growth and grazing rates (Table S7).

In the beginning of the production cycle, simulations revealed low predation rates (Fig. 2b). Changes in mixing conditions, affecting light and nutrient availability, may disrupt prey-predator relationships and allow populations to bloom during spring (Irigoien et al., 2005). This can be triggered by the poor nutritional status of the prey which alleviates grazing pressure (Mitra & Flynn 2006; Polimene et al., 2015); in the model, however, the overall nutritional status (as indicated by elemental ratios) of the prey was high. This reflects the importance of mixotrophy in the mixoplankton, and the tight coupling of nutrient regeneration and primary production. The simulated spring bloom was dominated by diatoms, due to their ability to reach high growth rates (Litchman et al., 2007), and grazing by protozooplankton was higher than by mesozooplankton, as previously observed at L4 (Fileman et al., 2010). Micro-CMs followed the diatom bloom in the model, as previously observed for dinoflagellates within the North Atlantic (Barton et al., 2013); simulations showed that phagotrophy was key for the rise of micro-CMs (Fig. 3). Experimental studies have shown that the net growth of dinoflagellates can be higher when they are growing as mixotrophs as opposed to solely autotrophic nutrition, though this is highly variable among species (Hansen, 2011).

Predation pressure was high under stratified conditions (Fig. 2b), as previously observed in the Western English Channel (Fileman et al., 2002; Fileman et al., 2010), and mixoplankton dominated the protist assemblage (Figs. 2a and 3). Mixoplanktonic nanoflagellates (nano-CMs) can obtain nutrients feeding on bacteria which are enriched in N and P relative to C (Unrein et al., 2007; Mitra et al., 2014). Mixoplankton displaying acquired phototrophy (NCMs) peaked later in spring and persisted as stratification developed in the model (Fig. 1b). Certain species of NCMs (the specialists) are largely dependent on phototrophy, can photoacclimate, and thrive in turbulent waters, such as *Mesodinium rubrum* (Johnson et al., 2013; Moeller et al., 2016), while others (the generalist oligotrich ciliates) rely more on phagotrophy and therefore benefit from C gained from phototrophy during periods of low prey availability (Stoecker et al., 2017). These features match well with the observational data at L4, with specialist forms (mainly *M. rubrum*) peaking during spring and generalist forms (i.e., oligotrich ciliates) during summer (Fig. S10).

In the simulations, as stratification breaks down at the end of summer, predation pressure increased on nano-CMs (Fig. 2b). Selective grazing by ciliates and dinoflagellates can be an important factor shaping the diversity of nano-CMs during autumn (Johnson et al., 2018). Once the water column is fully mixed, simulations revealed protist populations largely controlled by predation, and phagotrophs dominated the protist assemblage (Fig. 2). Predation pressure decreased throughout the winter, as supported by previous empirical studies close to L4 station (Fileman, personal communication). Nano-CMs found a window of opportunity during this period through the acquisition of carbon through phagotrophy (Fig. 3); therefore, our model captures also the scenario in which mixoplanktonic activity functions as a source of carbon under light-limited conditions (Czypionka et al., 2011; Vargas et al., 2012).

## 4.2 Mixoplankton functional differences explain carbon fluxes

Understanding the ecological roles of mixoplankton is of particular importance to biogeochemical cycling in the oceans (Mitra et al., 2014; Worden et al., 2015). Previous modelling studies have indicated that mixoplanktonic activity can significantly increase the production of dissolved organic carbon (DOC), nutrient cycling, as well as the trophic transfer and vertical export of carbon (Stickney et al., 2000; Mitra et al., 2014; Ward & Follows 2016). However, few studies have explored the role of different MFTs (Hammer & Pitchford 2005; Ghyoot et al., 2017; Leles et al., 2018).

Here, we show that the simulation of many carbon fluxes is strongly dependent on how and which MFTs are described in the model (Figs. 4 and 5). In a coastal temperate sea, a shift towards smaller primary producers in the absence of nano-CMs (Fig. 4) was responsible for the major changes observed in carbon fluxes (Fig. 5). Consequently, the model underestimates the recognised importance of mixoplankton as consumers of bacterial populations in oligotrophic and eutrophic conditions (Unrein et al., 2007; Zubkov and Tarran, 2008; Czepionka et al., 2011; Vargas et al., 2012). While the trophic transfer of carbon decreased substantially in the absence of nano-CMs, the contrary was observed when micro-CMs were not included in the model because diatoms biomass increased. Although not addressed in our study, micro-CMs might disrupt food webs in coastal eutrophic systems through the formation of harmful algal blooms (Gentien et al., 2007; Johnson et al., 2013). NCMs had low impact in carbon fluxes in our modelling experiments (Fig. 5). The contribution of NCMs to primary production was probably underestimated in our model since we simulated only generalist forms (Mitra et al., 2016). Specialist NCMs, particularly Rhizarians, can contribute substantially to primary production by harbouring symbiotic algae, with the potential to increase trophic transfer in the oligotrophic open oceans due to their large cell sizes (Stoecker et al., 2017). *Mesodinium*, another important common specialist NCM, was also not simulated. Therefore, our results strongly suggest that the impact of mixoplankton in carbon cycling is dependent on the composition of the mixoplanktonic community, and different types may be expected to play major roles in contrasting ecosystems (Stoecker et al., 2017).

While our results support the hypothesis that mixoplankton impact community size structure (Ward and Follows 2016), more importantly we show that the MFTs included in the model matter; these inclusions have profound consequences for how carbon is transferred between trophic levels. Thus, we show that despite having the same cell size, micro-CMs and NCMs have very different roles in carbon cycling (Fig. 5). The relative contribution of phototrophy and phagotrophy to mixoplankton growth is not simply correlated with cell size, but depends mainly on their ability (or not) to possess/maintain their own photosystems (Fig. 3; Adolf et al., 2006; Schoener and McManus, 2017). Allometric models that represent a continuum of size classes and different MFTs could provide further insights into the roles of mixoplankton in community dynamics and carbon cycling. What is clear is that mixoplanktonic activity provides a critical lynchpin in system dynamics in the model, a situation that is most likely mirrored in other locations, consistent with the biogeographic dominance of MFTs (Leles et al., 2017, 2019).

## 4.3 Putting mixoplankton on the spotlight: challenges and future directions

Our study suggests that recognizing functional differences through the representation of different MFTs help explain why mixoplankton can fill a great diversity of ecological niches. While mixoplanktonic activity is commonly perceived as being of greater importance during the temperate summer (Bruggeman, 2009; Berge et al., 2017; Chakraborty et al.,

2017), our results show that mixoplankton are active throughout the year. This was demonstrated here by a plankton ecosystem model validated against a 9yr time-series dataset for a coastal temperate sea. Overall, simulations agreed with observational data, performing better or at least as well as the ERSEM model upon which our model was based, and which does not describe mixoplankton (Figs. S4 and S5). In particular, mixoplankton could correct for the overestimated picophytoplankton biomass simulated by ERSEM at L4 (Fig. S4).

Our model does not account for lateral fluxes of nutrients and biota, which are known to play a role at the L4 station; for instance, signatures of riverine water are sometimes found (Smyth et al., 2010). This can help to explain why micro-CMs peaked earlier than expected at L4. It would also affect the simulation of mesozooplankton and thence of spring-diatom growth, which was overestimated by the model, driving the micro-CM peak (see also Supporting Text). Also, mesozooplankton appear first than their diatom-prey in the beginning of the production cycle at L4 (Atkinson et al., 2018) and this is not reproduced by our model (nor by ERSEM; Fig. S4). Other factors, such as diel vertical migration associated to shear-rate-modulated mortality can also influence micro-CMs dynamics and were not considered in the model (Gentien et al., 2007). This behaviour has been observed for *Karenia mikimotoi*, which is a dominant species at L4 (Widdicombe et al., 2010).

Although we used an exceptional dataset to evaluate our simulations, we acknowledge that one of the biggest challenges on modelling mixoplankton is the availability of data to evaluate their balance between phototrophic and phagotrophic nutrition as this is a function of both species identity and environmental conditions. So far, few empirical studies have estimated this balance to the carbon budgets of mixoplankton (Table S8). Our simulated values are within the range of values observed in the literature; however, these studies are species-specific and are based upon experimental conditions which differ among studies (e.g., temperature, light, nutrient, and prey conditions). Considering the diverse mixotrophic strategies adopted by protists, including within functional types (Table S8), further studies are necessary to estimate not only carbon but also nitrogen and phosphorus budgets (Carvalho and Granéli, 2010; Lin et al., 2018). These studies will require plankton ecologists to develop new methodologies, which will potentially involve the combination of different techniques, to quantify mixoplanktonic activity both under controlled conditions in the laboratory and within natural assemblages in the field (Worden et al., 2015; Beisner et al., 2019; Flynn et al., 2019).

Another important comment on modelling functional diversity is that incorporating diverse mixoplankton within ecosystem models is challenging due to competitive exclusion (Leles et al., 2018). Future studies focusing on the competitive abilities between, for example, nano-CMs and heterotrophic nanoflagellates can improve our understanding of their ecological niches (Edwards, 2019; Anschütz and Flynn, 2020). Similarly, we could not explore the different niches occupied by specialist versus generalist non-constitutive forms, as suggested by previous modelling studies (Moeller et al., 2016; Leles et al., 2018), because these did not coexist in our model. This is particularly relevant to test the hypothesis that the biogeography of acquired phototrophs vary according to their control over acquired phototrophy (Leles et al., 2017; Faure et al., 2019), but likely also relates to differences in prey preferences. These, combined with datasets that target mixoplankton, will allow us to advance our understanding of the role of these organisms in community assembly and ecosystem functioning in the oceans.

## 5. Conclusions

Our study show how mixoplankton of different forms are present over time and across depth in temperate seas. We achieved this by assigning their functional differences through the description of constitutive and non-constitutive forms, of different size classes, and how their phototrophy to phagotrophy ratios respond to environmental variability. We showed that seasonal population dynamics differ among the different functional types of mixoplankton. Our model captures the importance of photo-phago-trophy as a nutritional route not only during stratified conditions but also as a carbon source during light limitation. Moreover, our findings suggest that functional differences help us understand the diverse roles of mixoplanktonic assemblages in carbon cycling. While our study focused on temperate seas, further studies are needed in other marine ecosystems where mixoplanktonic assemblages are expected to differ (e.g., harmful algal blooms vs upwelling events vs stratified open oceans). Ultimately, incorporating functional diversity within 3D models will help to better elucidate the role of mixoplankton in biogeochemical cycling in the global oceans.

## Acknowledgements

The L4 long-term time series is part of the Western Channel Observatory which is funded as part of the NERC National Capability Programme. We thank the PML crew of Plymouth Quest and the PML staff involved in sampling and processing L4 data. Nutrient data were analysed by Carolyn Harris and Malcolm Woodward and plankton data were analysed by Claire Widdicombe, Glen Tarran, and Angus Atkinson. SGL is also grateful for the valuable discussions about L4 dynamics with Elaine Fileman, Angus Atkinson, Louise Cornwell, Helen Powley, and the PML ecosystem modelling team.

SGL was supported by the Brazilian government programme Science Without Borders through CNPq (Conselho Nacional de Desenvolvimento Científico e Tecnológico). LP was funded through the UK NERC grants NE/N001974/1 and NE/R011087/1. JBl, JBr and LP were supported by the NERC single centre national capability programme – Climate Linked Atlantic Sector Science (NE/R015953/1), contributing to Theme 4 - Fixed Point Observations (Western Channel Observatory) and Theme 5 Numerical modelling. AM and KJF were supported by the H2020-MSCA-ITN MixITiN Project 766327.

## References

- Adolf, J.E., Stoecker, D.K. & Harding, L.W. (2006). The balance of autotrophy and heterotrophy during mixotrophic growth of *Karlodinium micrum* (Dinophyceae). *J. Plankton Res.*, 28, 737–751. <https://doi.org/10.1093/plankt/fbl007>
- Anschütz, A.A. & Flynn, K.J. (2020). Niche separation between different functional types of mixoplankton: results from NPZ-style N-based model simulations. *Mar. Biol.*, 167:3. <https://doi.org/10.1007/s00227-019-3612-3>
- Atkinson, A., Harmer, R.A., Widdicombe, C.E., McEvoy, A.J., Smyth, T.J., Cummings, D.G., et al., (2015). Questioning the role of phenology shifts and trophic mismatching in a planktonic food web. *Prog. Oceanogr.*, 137, 498–512. <https://doi.org/10.1016/j.pocean.2015.04.023>
- Atkinson, A., Polimene, L., Fileman, E.S., Widdicombe, C.E., McEvoy, A.J., Smyth, T.J., et al., (2018). Comment. What drives plankton seasonality in a stratifying shelf sea? Some competing and complementary theories. *Limnol. Oceanogr.*, 63, 2877–2884. <https://doi.org/10.1002/lno.11036>
- Barton, A.D., Finkel, Z. V, Ward, B.A., Johns, D.G. & Follows, M.J. (2013). On the roles of cell size and trophic strategy in North Atlantic diatom and dinoflagellate communities. *Limnol. Oceanogr.*, 58, 254–266. <https://doi.org/10.4319/lo.2013.58.1.0254>
- Beisner, B.E., Grossart, H.-P. & Gasol, J.M. (2019). A guide to methods for estimating phago-mixotrophy in nanophytoplankton. *J. Plankton Res.*, 41, 77–89. <https://doi.org/10.1093/plankt/fbz008>
- Berge, T., Chakraborty, S., Hansen, P.J. & Andersen, K.H. (2017). Modeling succession of key resource-harvesting traits of mixotrophic plankton. *ISME J.*, 11, 212–223. <https://doi.org/10.1038/ismej.2016.92>
- Bird, D.F., Kalf, J. (1986). Bacterial grazing by planktonic lake algae. *Science*, 231, 493–495. DOI: 1126/science.231.4737.493
- Blackford, J.C., Allen, J.I. & Gilbert, F.J. (2004). Ecosystem dynamics at six contrasting sites: a generic modelling study. *J. Mar. Syst.*, 52, 191–215. <https://doi.org/10.1016/j.jmarsys.2004.02.004>
- Blondel, J. (2003). Guilds or functional groups: does it matter? *Oikos*, 100: 223–231. <https://doi.org/10.1034/j.1600-0706.2003.12152.x>
- Bruggeman, J. (2009). *Succession in plankton communities: a trait-based perspective*. Gildeprint Drukkerijen, Amsterdam.
- Burchard, H., Bolding, K. & Villarreal, M. (1999). *GOTM, a general ocean turbulence model. Theory, implementation and test cases. Technical Report EUR 18745 EN, European Commission*.
- Butenschön, M., Clark, J., Aldridge, J.N., Icarus Allen, J., Artioli, Y., Blackford, J., et al., (2016). ERSEM 15.06: A generic model for marine biogeochemistry and the ecosystem dynamics of the lower trophic levels. *Geosci. Model Dev.*, 9, 1293–1339. <https://doi.org/10.5194/gmd-9-1293-2016>
- Calbet, A. (2001). Mesozooplankton grazing effect on primary production: A global comparative analysis in marine ecosystems. *Limnol. Oceanogr.*, 46, 1824–1830.

- 559 <https://doi.org/10.4319/lo.2001.46.7.1824>
- 560 Caron, D.A., Sanders, R.W., Lim, E.L., Marrasé, C., Amaral, L.A., Whitney, S., et al.,  
561 (1993). Light-dependent phagotrophy in the freshwater mixotrophic chrysophyte  
562 *Dinobryon cylindricum*. *Microb. Ecol.*, 25, 93–111. <https://doi.org/10.1007/BF00182132>
- 563 Carvalho, W.F. & Granéli, E. (2010). Contribution of phagotrophy versus autotrophy to  
564 *Prymnesium parvum* growth under nitrogen and phosphorus sufficiency and deficiency.  
565 *Harmful Algae*, 9, 105–115. <https://doi.org/10.1016/j.hal.2009.08.007>
- 566 Chakraborty, S., Nielsen, L.T. & Andersen, K.H. (2017). Trophic Strategies of Unicellular  
567 Plankton. *Am. Nat.*, 189, E77–E90. <https://doi.org/10.1086/690764>
- 568 Chapin, F., Walker, B., Hobbs, R., Hooper, D., Lawton, J., Sala, O., et al., (1997). Biotic  
569 control over the functioning of ecosystems. *Science*, 277, 500–504.  
570 <https://doi.org/10.1126/science.277.5325.500>
- 571 Czypionka, T., Vargas, C.A., Silva, N., Daneri, G., González, H.E. & Iriarte, J.L. (2011).  
572 Importance of mixotrophic nanoplankton in Aysén Fjord (Southern Chile) during austral  
573 winter. *Cont. Shelf Res.*, 31, 216–224. <https://doi.org/10.1016/j.csr.2010.06.014>
- 574 Edwards, K.F. (2019). Mixotrophy in nanoflagellates across environmental gradients in the  
575 ocean. *Proc. Natl. Acad. Sci. U. S. A.*, 116, 6211–6220.  
576 <https://doi.org/10.1073/pnas.1814860116>
- 577 Faure, E., Not, F., Benoiston, A.S., Labadie, K., Bittner, L. & Ayata, S.D. (2019).  
578 Mixotrophic protists display contrasted biogeographies in the global ocean. *ISME J.*, 13,  
579 1072–1083. <https://doi.org/10.1038/s41396-018-0340-5>
- 580 Fileman, E., Petropavlovsky, A. & Harris, R. (2010). Grazing by the copepods *Calanus*  
581 *helgolandicus* and *Acartia clausi* on the protozooplankton community at station L4 in  
582 the Western English Channel. *J. Plankton Res.*, 32, 709–724.  
583 <https://doi.org/10.1093/plankt/fbp142>
- 584 Fileman, E.S., Cummings, D.G. & Llewellyn, C.A. (2002). Microplankton community  
585 structure and the impact of microzooplankton grazing during an *Emiliania huxleyi*  
586 bloom, off the Devon coast. *J. Mar. Biol. Assoc. United Kingdom*, 82, 359–368.  
587 <https://doi.org/10.1017/S0025315402005593>
- 588 Flynn, K.J. & Mitra, A. (2009). Building the “perfect beast”: Modelling mixotrophic  
589 plankton. *J. Plankton Res.*, 31, 965–992. <https://doi.org/10.1093/plankt/fbp044>
- 590 Flynn, K.J., Mitra, A., Anestis, K., Anschütz, A.A., Calbet, A., Ferreira, G.D., et al., (2019).  
591 Mixotrophic protists and a new paradigm for marine ecology: where does plankton  
592 research go now? *J. Plankton Res.*, 00, 1–17. <https://doi.org/10.1093/plankt/fbz026>
- 593 Flynn, K.J., Stoecker, D.K., Mitra, A., Raven, J.A., Glibert, P.M., Hansen, P.J., et al., (2013).  
594 Misuse of the phytoplankton-zooplankton dichotomy: The need to assign organisms as  
595 mixotrophs within plankton functional types. *J. Plankton Res.*, 35, 3–11.  
596 <https://doi.org/10.1093/plankt/fbs062>
- 597 Gentien, P., Lunven, M., Lazure, P., Youenou, A. & Crassous, M.. (2007). Motility and  
598 autotoxicity in *Karenia mikimotoi* (Dinophyceae). *Philos. Trans. R. Soc. B Biol. Sci.*,  
599 362, 1937–1946. <https://doi.org/10.1098/rstb.2007.2079>
- 600 Ghyoot, C., Lancelot, C., Flynn, K.J., Mitra, A. & Gypens, N. (2017). Introducing



- 601 mixotrophy into a biogeochemical model describing an eutrophied coastal ecosystem:  
 602 The Southern North Sea. *Prog. Oceanogr.*, 157, 1–11.  
 603 <https://doi.org/10.1016/j.pocean.2017.08.002>
- 604 Gran-Stadniczeñko, S., Egge, E., Hostyeva, V., Logares, R., Eikrem, W. & Edvardsen, B.  
 605 (2019). Protist Diversity and Seasonal Dynamics in Skagerrak Plankton Communities as  
 606 Revealed by Metabarcoding and Microscopy. *J. Eukaryot. Microbiol.*, 66, 494–513.  
 607 <https://doi.org/10.1111/jeu.12700>
- 608 Hammer, A.C. & Pitchford, J.W. (2005). The role of mixotrophy in plankton bloom  
 609 dynamics, and the consequences for productivity. *ICES J. Mar. Sci.*, 62, 833–840.  
 610 <https://doi.org/10.1016/j.icesjms.2005.03.001>
- 611 Hansell, D.A. (2013). Recalcitrant Dissolved Organic Carbon Fractions. *Ann. Rev. Mar. Sci.*,  
 612 5, 421–445. <https://doi.org/10.1146/annurev-marine-120710-100757>
- 613 Hansen, P.J. (2011). The Role of Photosynthesis and Food Uptake for the Growth of Marine  
 614 Mixotrophic Dinoflagellates. *J. Eukaryot. Microbiol.*, 58, 203–214.  
 615 <https://doi.org/10.1111/j.1550-7408.2011.00537.x>
- 616 Hansson, T.H., Grossart, H.-P., del Giorgio, P.A., St-Gelais, N.F. & Beisner, B.E. (2019).  
 617 Environmental drivers of mixotrophs in boreal lakes. *Limnol. Oceanogr.*, 64, 1688–  
 618 1705. <https://doi.org/10.1002/lno.11144>
- 619 Irigoien, X., Flynn, K.J. & Harris, R.P. (2005). Phytoplankton blooms: A “loophole” in  
 620 microzooplankton grazing impact? *J. Plankton Res.*, 27, 313–321.  
 621 <https://doi.org/10.1093/plankt/fbi011>
- 622 Johnson, M.D., Beaudoin, D.J., Frada, M.J., Brownlee, E.F. & Stoecker, D.K. (2018). High  
 623 Grazing Rates on Cryptophyte Algae in Chesapeake Bay. *Front. Mar. Sci.*, 5, 1–13.  
 624 <https://doi.org/10.3389/fmars.2018.00241>
- 625 Johnson, M.D., Stoecker, D.K. & Marshall, H.G. (2013). Seasonal dynamics of *Mesodinium*  
 626 *rubrum* in Chesapeake Bay. *J. Plankton Res.*, 35, 877–893.  
 627 <https://doi.org/10.1093/plankt/fbt028>
- 628 Jolliff, J.K., Kindle, J.C., Shulman, I., Penta, B., Friedrichs, M.A.M., Helber, R., et al.,  
 629 (2009). Summary diagrams for coupled hydrodynamic-ecosystem model skill  
 630 assessment. *J. Mar. Syst.*, 76, 64–82. <https://doi.org/10.1016/j.jmarsys.2008.05.014>
- 631 Leles, S.G., Mitra, A., Flynn, K.J., Stoecker, D.K., Hansen, P.J., Calbet, A., et al., (2017).  
 632 Oceanic protists with different forms of acquired phototrophy display contrasting  
 633 biogeographies and abundance. *Proc. R. Soc. B*, 284, 20170664.  
 634 <https://doi.org/10.1098/rspb.2017.0664>
- 635 Leles, S.G., Mitra, A., Flynn, K.J., Tillmann, U., Stoecker, D., Jeong, H.J., et al., (2019).  
 636 Sampling bias misrepresents the biogeographical significance of constitutive mixotrophs  
 637 across global oceans. *Glob. Ecol. Biogeogr.*, 28, 418–428.  
 638 <https://doi.org/10.1111/geb.12853>
- 639 Leles, S.G., Polimene, L., Bruggeman, J., Blackford, J., Ciavatta, S., Mitra, A., et al., (2018).  
 640 Modelling mixotrophic functional diversity and implications for ecosystem function. *J.*  
 641 *Plankton Res.*, 40, 627–642. <https://doi.org/10.1093/plankt/fby044>
- 642 Lin, C-H., Flynn, K.J., Mitra, A. & Glibert, P.M. (2018). Simulating effects of variable  
 643 stoichiometry and temperature on mixotrophy in the harmful dinoflagellate *Karlodinium*

- 644 *veneficum*. *Frontiers Mar. Sci.*, 5, 320. <https://doi.org/10.3389/fmars.2018.00320>
- 645 Litchman, E., Klausmeier, C.A., Schofield, O.M. & Falkowski, P.G. (2007). The role of  
646 functional traits and trade-offs in structuring phytoplankton communities: scaling from  
647 cellular to ecosystem level. *Ecol. Lett.*, 10, 1170–1181. [https://doi.org/10.1111/j.1461-](https://doi.org/10.1111/j.1461-0248.2007.01117.x)  
648 [0248.2007.01117.x](https://doi.org/10.1111/j.1461-0248.2007.01117.x)
- 649 Margalef, R. (1978). Life-forms of phytoplankton as survival alternatives in an unstable  
650 environment. *Ocean. Acta*, 1, 493–509.
- 651 McManus, G.B., Schoener, D.M. & Haberlandt, K. (2012). Chloroplast symbiosis in a marine  
652 ciliate: ecophysiology and the risks and rewards of hosting foreign organelles. *Front.*  
653 *Microbiol.*, 3, 321. <https://doi.org/10.3389/fmicb.2012.00321>
- 654 Mitra, A. & Flynn, K.J. (2006) Promotion of harmful algal blooms by zooplankton predatory  
655 activity. *Biology Letters*, 2, 194–197. <https://doi.org/10.1098/rsbl.2006.0447>
- 656 Mitra, A. & Flynn, K.J. (2010). Modelling mixotrophy in harmful algal blooms: more or less  
657 the sum of the parts? *J. Mar. Syst.*, 83, 158–169.  
658 <https://doi.org/10.1016/j.jmarsys.2010.04.006>
- 659 Mitra, A., Flynn, K.J., Burkholder, J.M., Berge, T., Calbet, A., Raven, J.A., et al., (2014).  
660 The role of mixotrophic protists in the biological carbon pump. *Biogeosciences*, 11,  
661 995–1005. <https://doi.org/10.5194/bg-11-995-2014>
- 662 Mitra, A., Flynn, K.J., Tillmann, U., Raven, J.A., Caron, D., Stoecker, D.K., et al., (2016).  
663 Defining Planktonic Protist Functional Groups on Mechanisms for Energy and Nutrient  
664 Acquisition: Incorporation of Diverse Mixotrophic Strategies. *Protist*, 167, 106–120.  
665 <https://doi.org/10.1016/j.protis.2016.01.003>
- 666 Moeller, H. V., Peltomaa, E., Johnson, M.D. & Neubert, M.G. (2016). Acquired phototrophy  
667 stabilises coexistence and shapes intrinsic dynamics of an intraguild predator and its  
668 prey. *Ecol. Lett.*, 19, 393–402. <https://doi.org/10.1111/ele.12572>
- 669 Polimene, L., Mitra, A., Sailley, S.F., Ciavatta, S., Widdicombe, C.E., Atkinson, A., et al.,  
670 (2015). Decrease in diatom palatability contributes to bloom formation in the Western  
671 English Channel. *Prog. Oceanogr.*, 137, 484–497.  
672 <https://doi.org/10.1016/j.pocean.2015.04.026>
- 673 Schoener, D.M. & McManus, G.B. (2017). Growth, grazing, and inorganic C and N uptake in  
674 a mixotrophic and a heterotrophic ciliate. *J. Plankton Res.*, 39, 379–391.  
675 <https://doi.org/10.1093/plankt/fbx014>
- 676 Selosse, M.-A., Charpin, M. & Not, F. (2017). Mixotrophy everywhere on land and in water:  
677 the grand écart hypothesis. *Ecol. Lett.*, 20, 246–263. <https://doi.org/10.1111/ele.12714>
- 678 Smyth, T.J., Fishwick, J.R., Al-Moosawi, L., Cummings, D.G., Harris, C., Kitidis, V., et al.,  
679 (2010). A broad spatio-temporal view of the Western English Channel observatory. *J.*  
680 *Plankton Res.*, 32, 585–601. <https://doi.org/10.1093/plankt/fbp128>
- 681 Sommer, U., Adrian, R., De Senerpont Domis, L., Elser, J.J., Gaedke, U., Ibelings, B., et al.,  
682 (2012). Beyond the Plankton Ecology Group (PEG) Model: Mechanisms Driving  
683 Plankton Succession. *Annu. Rev. Ecol. Evol. Syst.*, 43, 429–448.  
684 <https://doi.org/10.1146/annurev-ecolsys-110411-160251>
- 685 Sterner, R.W. (1989). The role of grazers in Phytoplankton Succession. In: *Plankton Ecology*,

- 686 ed. Sommer, U. Springer-Verlag Berlin Heidelberg, pp. 107–170.
- 687 Stickney, H.L., Hood, R.R. & Stoecker, D.K. (2000). The impact of mixotrophy on  
688 planktonic marine ecosystems. *Ecol. Model.*, 125: 203–230.  
689 [https://doi.org/10.1016/S0304-3800\(99\)00181-7](https://doi.org/10.1016/S0304-3800(99)00181-7)
- 690 Stoecker, D., Hansen, P., Caron, D. & Mitra, A. (2017). Mixotrophy in the marine plankton.  
691 *Ann. Rev. Mar. Sci.*, 9, 311–335. [https://doi.org/10.1146/annurev-marine-010816-](https://doi.org/10.1146/annurev-marine-010816-060617)  
692 060617
- 693 Stoecker, D.K., Michaels, A.E. & Davis, L.H. (1987). Large proportion of marine planktonic  
694 ciliates found to contain functional chloroplasts. *Nature*, 326, 790–792.  
695 <https://doi.org/10.1038/326790a0>
- 696 Tarran, G.A. & Bruun, J.T. (2015). Nanoplankton and picoplankton in the Western English  
697 Channel: Abundance and seasonality from 2007–2013. *Prog. Oceanogr.*, 137, 446–455.  
698 <https://doi.org/10.1016/j.pocean.2015.04.024>
- 699 Tittel, J., Bissinger, V., Zippel, B., Gaedke, U., Bell, E., Lorke, A., et al., (2003). Mixotrophs  
700 combine resource use to outcompete specialists: implications for aquatic food webs.  
701 *Proc. Natl. Acad. Sci. U. S. A.*, 100, 12776–12781.  
702 <https://doi.org/10.1073/pnas.2130696100>
- 703 Troost, T.A., Kooi, B.W. & Kooijman, S.A.L.M. (2005). Ecological Specialization of  
704 Mixotrophic Plankton in a Mixed Water Column. *Am. Nat.*, 166, E45–E61.  
705 <https://doi.org/10.1086/432038>
- 706 Unrein, F., Massana, R., Alonso-Sáez, L. & Gasol, J.M. (2007). Significant year-round effect  
707 of small mixotrophic flagellates on bacterioplankton in an oligotrophic coastal system.  
708 *Limnol. Oceanogr.*, 52, 456–469. <https://doi.org/10.4319/lo.2007.52.1.0456>
- 709 Vargas, C., Contreras, P. & Iriarte, J. (2012). Relative importance of phototrophic,  
710 heterotrophic, and mixotrophic nanoflagellates in the microbial food web of a river-  
711 influenced coastal upwelling area. *Aquat. Microb. Ecol.*, 65, 233–248.  
712 <https://doi.org/10.3354/ame01551>
- 713 Ward, B.A. & Follows, M.J. (2016). Marine mixotrophy increases trophic transfer efficiency,  
714 mean organism size, and vertical carbon flux. *Proc. Natl. Acad. Sci. U. S. A.*, 113, 2958–  
715 2963. <https://doi.org/10.1073/pnas.1517118113>
- 716 Weithoff, G. & Beisner, B.E. (2019). Measures and Approaches in Trait-Based  
717 Phytoplankton Community Ecology – From Freshwater to Marine Ecosystems. *Front.*  
718 *Mar. Sci.*, 6, 1–11. <https://doi.org/10.3389/fmars.2019.00040>
- 719 Widdicombe, C.E., Eloire, D., Harbour, D., Harris, R.P. & Somerfield, P.J. (2010). Long-  
720 term phytoplankton community dynamics in the Western English Channel. *J. Plankton*  
721 *Res.*, 32, 643–655. <https://doi.org/10.1093/plankt/fbp127>
- 722 Wilken, S., Huisman, J., Naus-Wiezer, S. & Donk, V. (2013). Mixotrophic organisms  
723 become more heterotrophic with rising temperature. *Ecol. Lett.*, 16: 225–233.  
724 <https://doi.org/10.1111/ele.12033>
- 725 Worden, A.Z., Follows, M.J., Giovannoni, S.J., Wilken, S., Zimmerman, A.E. & Keeling,  
726 P.J. (2015). Rethinking the marine carbon cycle: Factoring in the multifarious lifestyles  
727 of microbes. *Science*, 347, 1257594. <https://doi.org/10.1126/science.1257594>

728 Zubkov, M. V & Tarran, G.A. (2008). High bacterivory by the smallest phytoplankton in the  
729 North Atlantic Ocean. *Nature*, 455, 224–226. <https://doi.org/10.1038/nature07236>

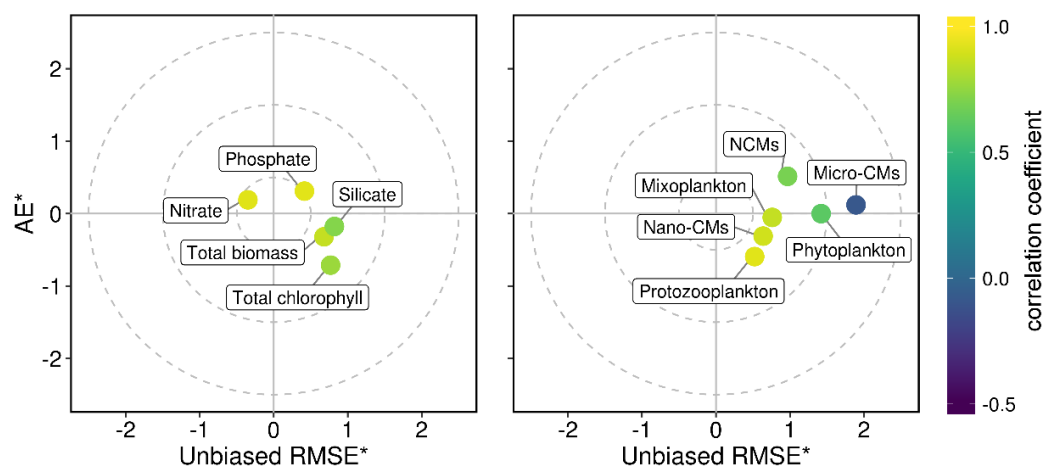
730

731 **Supporting Information**

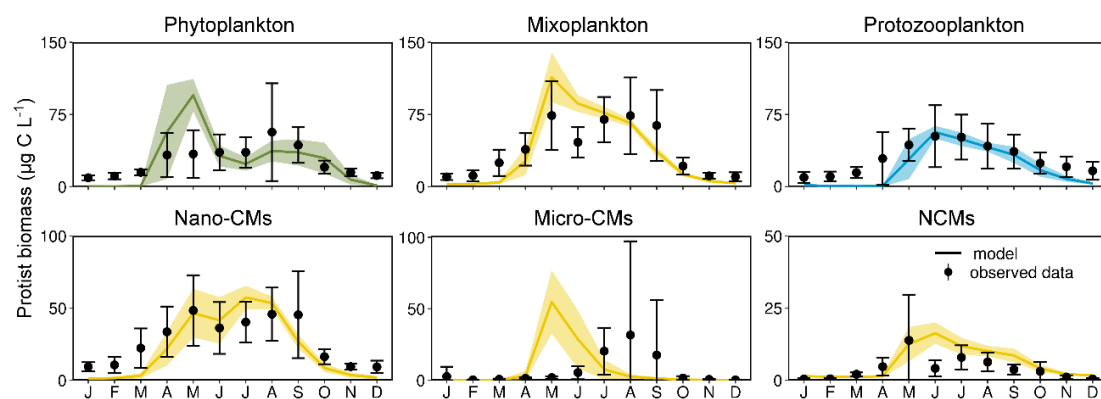
732 Additional supporting information may be downloaded via the online version of this article.

733 **Figures**

(a)



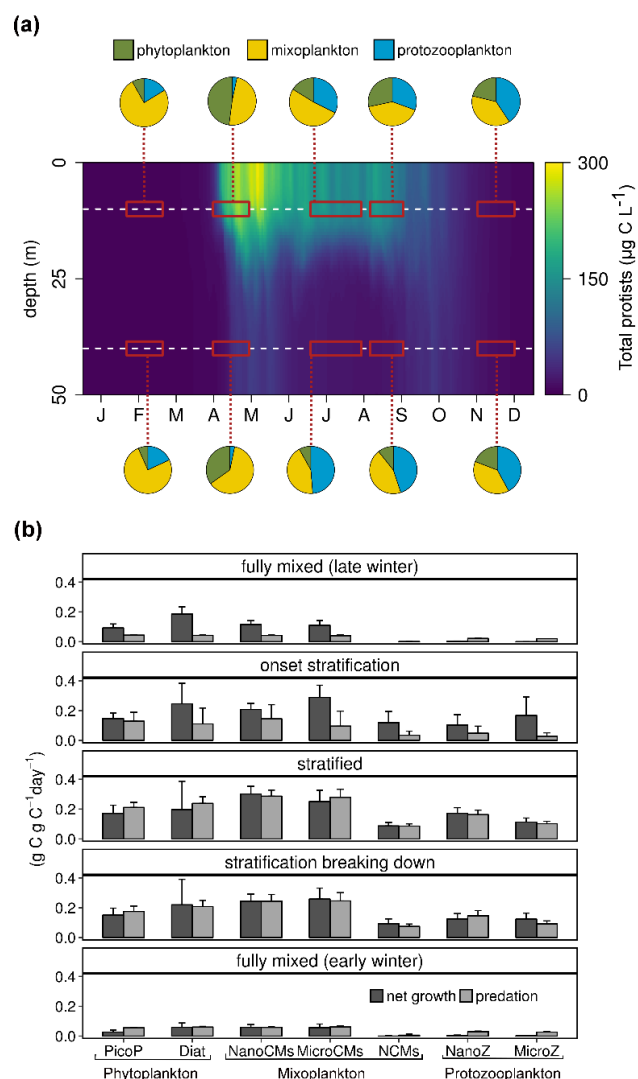
(b)



734

735 **Figure 1** Model validation against climatological data at L4 station (at 10 m depth) showing  
 736 (a) target diagrams with the normalised average error (AE\*, abscissa), the normalised and  
 737 unbiased root mean squared error (RMSE\*, ordinate), and the correlation coefficient (colour  
 738 code) for inorganic nutrients, total chlorophyll, and plankton biomass and (b) seasonal  
 739 evolution of protist biomass; phytoplankton, mixoplankton, and protozooplankton are given  
 740 in the upper panels and different mixoplankton functional types (nano-CMs, micro-CMs, and  
 741 NCMs) are given in the lower panels (lines – simulations; dots – observations). Mean ( $\pm$ SD)  
 742 values correspond to the period 2006–2014. Nano-CMs – constitutive mixoplankton within  
 743 the nanoplankton size spectrum; Micro-CMs – constitutive mixoplankton within the  
 744 microplankton size spectrum; NCMs – non-constitutive mixoplankton within the  
 745 microplankton size spectrum.

746



747

748 **Figure 2** Simulated seasonal succession of protist trophic strategies at L4 given by (a) the  
 749 relative contribution of phytoplankton (green), mixoplankton (yellow), and protozooplankton  
 750 (blue) to total protist biomass and (b) growth (black) and predation (grey) rates at 10 m for  
 751 each functional type as a measure of population fitness. Data are given for selected time  
 752 periods and depth. Mean ( $\pm$ SD) values correspond to the period 2006–2014. PicoP –  
 753 picophytoplankton. Nano-CMs – constitutive mixoplankton (nanoplankton size spectrum);  
 754 Diat – diatoms; micro-CMs – constitutive mixoplankton (microplankton size spectrum);  
 755 NCMs – non-constitutive mixoplankton (microplankton size spectrum); NanoZ – nano-  
 756 protozooplankton; MicroZ – micro-protozooplankton.

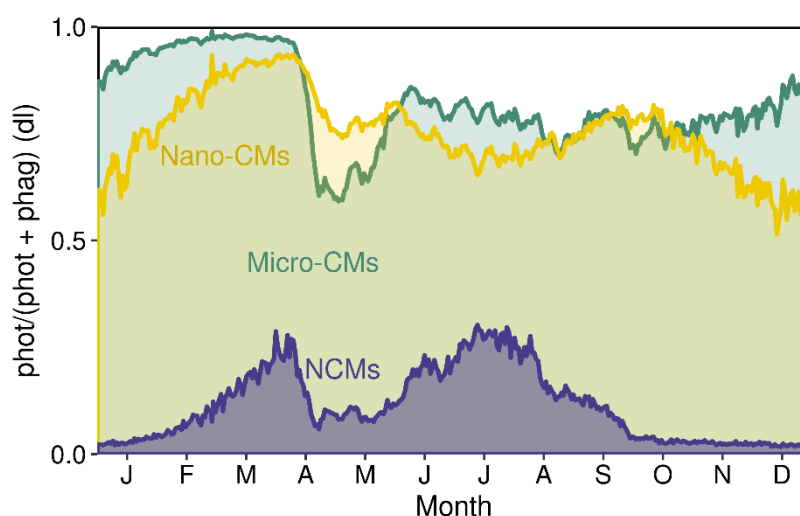


**Figure 3** The ratio between carbon fixation (phototrophy) and the total carbon uptake (phototrophy + phagotrophy) rates among different mixoplankton functional types over the seasonal cycle at L4 (at 10 m depth). Mean values correspond to the period 2006–2014; phot – phototrophy; phag – phagotrophy; dl – dimensionless. Nano-CMs – constitutive mixoplankton (nanoplankton size spectrum); Micro-CMs – constitutive mixoplankton (microplankton size spectrum); NCMs – non-constitutive mixoplankton (microplankton size spectrum).

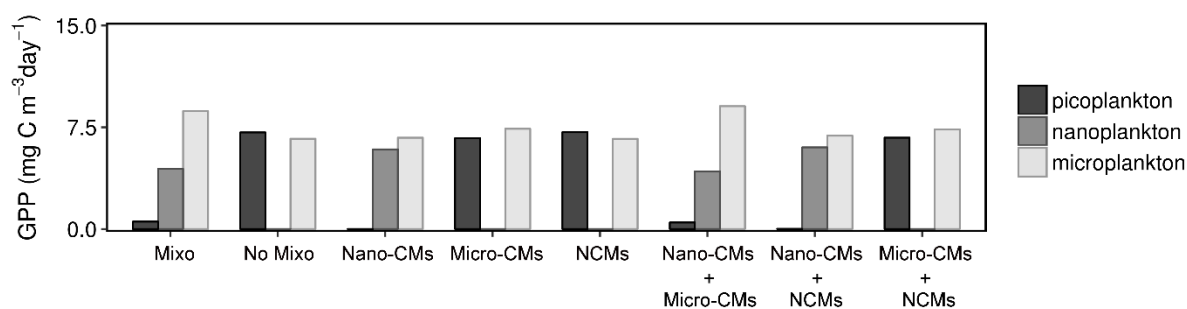


**Figure 4** Partitioning of gross primary production (GPP) among different size-classes (picoplankton, nanoplankton, microplankton). The model used in the present study, accounting for nano-CMs, micro-CMs and NCMs (Mixo), is compared against simulations which accounted for none (No Mixo), one, or two mixoplankton functional types. GPP values were averaged over the year and integrated over the water column. Nano-CMs – constitutive mixoplankton (nanoplankton size spectrum); Micro-CMs – constitutive mixoplankton (microplankton size spectrum); NCMs – non-constitutive mixoplankton (microplankton size spectrum).

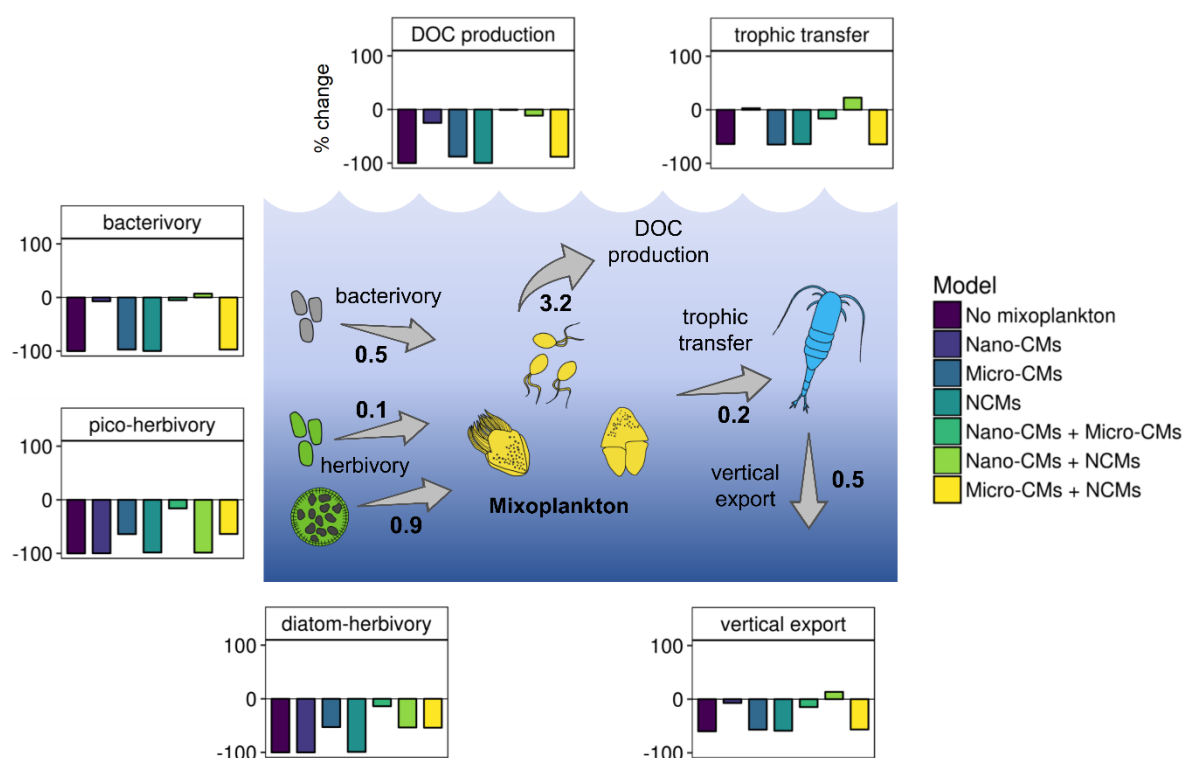


**Figure 5** Ecological roles of mixoplanktonic communities in the carbon cycling within temperate seas showing: carbon fluxes (mg C m<sup>-3</sup> day<sup>-1</sup>) estimated once nano-CMs, micro-CMs and NCMs are modelled (central schematic) and the % of flux change once simulations accounted for none, one, or two mixoplankton functional types (see colour-legend). Values were averaged over the year and integrated over the water column. DOC – dissolved organic carbon; pico – picophytoplankton; Nano-CMs – constitutive mixoplankton (nanoplankton



786 size spectrum); Micro-CMs – constitutive mixoplankton (microplankton size spectrum);  
787 NCMs – non-constitutive mixoplankton (microplankton size spectrum).  
788